ACS Catalysis

Research Article

pubs.acs.org/acscatalysis

Mesoporous Silica Materials Labeled for Optical Oxygen Sensing and Their Application to Development of a Silica-Supported Oxidoreductase Biocatalyst

Juan M. Bolivar,[¶] Sabine Schelch,[¶] Torsten Mayr,[⊥] and Bernd Nidetzky*[,¶,‡]

[¶]Institute of Biotechnology and Biochemical Engineering, Graz University of Technology, NAWI Graz, Petersgasse 12, A-8010 Graz, Austria

[⊥]Institute of Analytical Chemistry and Food Chemistry, Graz University of Technology, NAWI Graz, Stremayrgasse 9, A-8010 Graz, Austria

[‡]Austrian Centre of Industrial Biotechnology (acib), Petersgasse 14, A-8010 Graz, Austria

Supporting Information

ABSTRACT: Porous silica materials make great supports for heterogeneous catalysis with immobilized enzymes; however, direct functionalization of their surface through stable attachment of enzymes, reporter molecules, or both is a difficult problem. Overcoming that is necessary for practical implementation. Here, we integrate the development of luminophor-doped oxygen-sensing silica materials with a modular strategy of enzyme immobilization to demonstrate generally applicable design of an oxygen-dependent biocatalyst on a porous silica support. Zbasic2, a highly positively charged silica-binding module of about 7 kDa size, was fused to D-amino acid oxidase, and the resulting chimeric protein was tethered noncovalently via Zbasic2 in defined orientation and in a highly selective manner on silica. The enzyme supports used differed in overall shape and size as well as in internal pore structure. A confocal laser scanning microscopy (CLSM) analysis that employed the oxidase's flavin cofactor as the fluorescent reporter group showed a homogeneous internal protein distribution in all supports used. Ru-based organometallic luminophor was adsorbed tightly onto the silica supports, thus enabling internal optical sensing of the O_2 available to the enzymatic reaction. Optimization of the surface labeling regarding homogeneous luminophor distribution was guided, and its efficacy was verified by CLSM. Mesostructured silica surpassed controlled pore glass by ≥10-fold in terms of immobilized enzyme effectiveness at high loading of oxidase activity. The effect was shown from detailed comparison of the time-resolved O_2 concentration profiles in solution and inside porous support to result exclusively from variable degrees of diffusion-caused limitation in the internal O_2 availability. Enzyme immobilized on mesostructured silica approached perfection of a heterogeneous biocatalyst in being almost as effective as the free enzyme (assayed in oxidative deamination of D-methionine), thus emphasizing the large benefit of targeted mass transfer intensification, through proper choice of support parameters, in the development of immobilizates of O_2-dependent oxidoreductases on porous silica material.

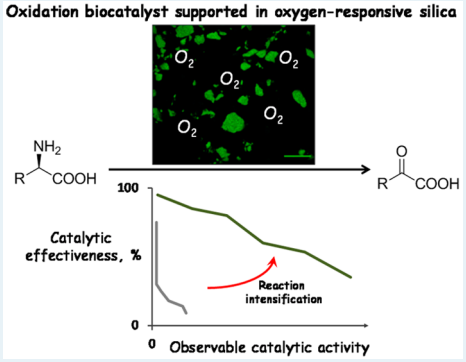

KEYWORDS: *biocatalysis, oxygen-dependent oxidations, silica materials, enzyme immobilization, fusion protein, silica binding module, optical sensing, intraparticle oxygen gradient*

INTRODUCTION

In the chemical sciences, the use of enzymes as synthetic catalysts is rapidly gaining in importance.[1,2] Like in chemocatalysis, enzyme-derived biocatalysts are categorized broadly according to their solubility in the reaction bulk into a homogeneous or heterogeneous class.[3−6] Generally, but especially when the scales get bigger, heterogeneous biocatalysts are preferred by virtue of their simplified recycling and all the advantages thus involved.[4,5,7] However, enzymes are normally very soluble in the water-based solvents they require for activity, stability, or both. Therefore, making enzymes insoluble constitutes a core task in the development of almost any heterogeneous biocatalyst, the process of which is generally referred to as immobilization.[5,7,8] There exist different principles of enzyme immobilization, but fixation on a solid support is the one most commonly used across scales.[5,8,9] The quest for a suitable support therefore presents a critical point of departure in virtually any enzyme immobilization, in which the decision made gives direction to the development chain as a whole.[6,9] In addition to creating strong opportunities for operating biocatalytic transformations continuously, immobilization on solid support often results in enhanced enzyme resistance to various forms of denaturation. This in turn also supports the transition from batch to continuous bioprocess-

Received: May 22, 2015
Published: August 28, 2015

DOI: 10.1021/acscatal.5b01601
ACS Catal. 2015, 5, 5984−5993

ing.[10−12] A suitably designed immobilization can also affect enzyme activity and selectivity in a positive way.[11]

Considering the chemical−morphological−mechanical−financial tetrad of criteria typically underlying the selection of immobilization supports, silica is expected to emerge as a top candidate, for it is highly biocompatible, readily adjustable in size, stable chemically and incompressible, and also relatively inexpensive.[6,13−15] However, it is noted that silica is not elastic, and like many other supports used for enzyme immobilization, it can therefore undergo some abrasion when stirred in suspension. The reason that silica is not widely used for enzyme immobilization at present is the difficulty in getting enzymes fixed on the silica surface in a *straightforward* and *practical* manner,[6,12−14,16] whereby chemical derivatization of the surface should be avoided. The availability of supports of a suitable internal pore structure used to be another limitation that has been largely overcome, however, through the recent advent of mesoporous silica materials.[12,17−20] Identification of protein-based silica binding modules (SBM)[21−25] and demonstration that fusion to SBM constituted a general strategy of designing enzyme chimeras with high affinity for becoming attached to silica surfaces presented significant progress in the task of making underivatized silica materials readily exploitable for enzyme immobilization.[22]

We have shown in recent work that Zbasic2, a strongly positively charged three-helix bundle of ∼7 kDa size, presents a highly efficient SBM for the immobilization of different enzymes, including the oxidase used herein and described later.[22,23] Protein attachment to the silica surface of controlled pore glass (CPG) occurred directed via the Zbasic2 module.[21,22] It was also highly selective under the stringent immobilization conditions used. Therefore, on offering crude bacterial cell extract for immobilization, it was essentially the target protein containing Zbasic2 that remained bound to the support. By virtue of its noncovalent nature, the Zbasic2-silica surface interaction could be tuned through variation in pH and salt concentration to switch from being quasi-irreversible during the enzymatic reaction to being readily reversible during regeneration of the support.[22] Finally, the multivalency of protein−surface interactions in homooligomeric Zbasic2_enzyme appeared to be useful not only for high-affinity binding but also for oligomer stabilization of the enzyme immobilized.[21] On the basis of these advances, the current study was undertaken to show systematic and comprehensive development of a highly effective O_2-dependent heterogeneous biocatalyst on silica support. Controllable and selective use of O_2 as the oxidant in synthetic transformations constitutes an important long-term objective within the chemical sciences.[26−35] A general strategy of creating immobilized enzyme catalysts for that purpose would therefore be highly relevant in the field.[36−39]

Development of an immobilized enzyme as a heterogeneous biocatalyst would strongly benefit from availability of a suitable process analytical technology.[7,13,40] Therefore, in addition to directed immobilization on silica via SBM, the current study has integrated a second line of recent research from this laboratory on immobilized enzymes, which is the application of optochemical sensing methods for the direct determination of the heterogeneous O_2 environment inside solid supports.[41−43] We have shown in earlier papers how significantly limited the activity of an immobilized oxidase can become as a result of reaction-caused depletion of the O_2 substrate within the solid support.[42,43] We have also shown that the degree of internal limitation in O_2 availability constitutes a parameter long sought-after in the rational design of immobilization supports for mass transfer-intensified conversions by O_2-dependent immobilized enzymes.[42,43] However, the supports used in our previous research were all of organic polymer materials, such as polymethacrylate. Therefore, a major aim of this study was the development of internally phosphorescently labeled silica materials suitable for O_2 sensing and application of these materials to time-resolved determination of the support internal O_2 concentration during heterogeneous enzymatic reactions. Thus, different silica materials differing in particle diameter and pore size could be evaluated directly regarding the effect of the support parameters on the degree of diffusional limitation. Using D-amino acid oxidase (from the yeast *Trigonopsis variabilis*; DAAO) as a representative and also well-known model enzyme,[21,37,44] three silica supports, CPG and the mesocellular silica foams MSU-VLP and MSU-F,[14,45] were examined, and the selection of the most effective one was demonstrated on the basis of the direct evaluation of the internal effects of slow O_2 diffusion. Briefly, DAAO is a FAD-dependent enzyme that catalyzes oxidative deamination of an α-D-amino acid substrate coupled to the reduction of O_2 into H_2O_2.[44,46] Acting on α-amino acids, DAAO has absolute (D compared to L) enantioselectivity and shows very broad side chain specificity, a combination of enzyme properties much desired for chiral synthesis of fine chemicals.[46,47] DAAO immobilized on mesostructured silica presented a unique case in which a heterogeneous O_2-dependent biocatalyst approached perfection in being virtually as effective as the free enzyme.

RESULTS AND DISCUSSION

Immobilization of DAAO on Mesoporous Silica Supports. The relevant properties of the silica supports used (CPG, MSU-VLP and MSU-F) are summarized in Tables S1, S2. In addition to differences in specific surface area and pore volume, the supports represented significant variation in particle size and pore diameter. Figure 1 and Figure S1 show the differences in particle size. For the purpose of this study, particle size and pore diameter were the key parameters, thus explaining the selection of the three supports. In addition, CPG is a very well defined "standard" silica support, and direct immobilization of Zbasic2 fusion proteins on it has been studied before. MSU-VLP and MSU-F are highly representative for an emerging class of mesoporous silica materials.[14,17] Note that geometrical properties of the supports are unaltered on changing from dry to wet conditions. The supports do not measurably swell up in water.

The previously described DAAO chimera that contains Zbasic2 N-terminally fused to the enzyme was used. Figure 2 shows results of immobilization of Zbasic2_DAAO (DAAO containing Zbasic2 fused as SBM to the enzyme's N-terminus) on the three silica supports. The immobilization was performed stepwise in which a protein concentration of 5 g/L was used in solution and an enzyme activity of 400 U (= μmol/min)/g_support was offered in each step. All at once loading was not used so as to avoid protein aggregation in solution and on the solid surface at high soluble protein concentration. In terms of the immobilization yield, that is, the part of the offered enzyme activity that was bound, and also the amount of protein loadable, MSU-F was superior to CPG and MSU-VLP, both of which had loading limits at ∼2500 U/g_support and 35 mg protein/g_support. With MSU-F, the immobilization yield was complete up to the maximum amount of activity loaded, and

DOI: 10.1021/acscatal.5b01601
ACS Catal. 2015, 5, 5984−5993

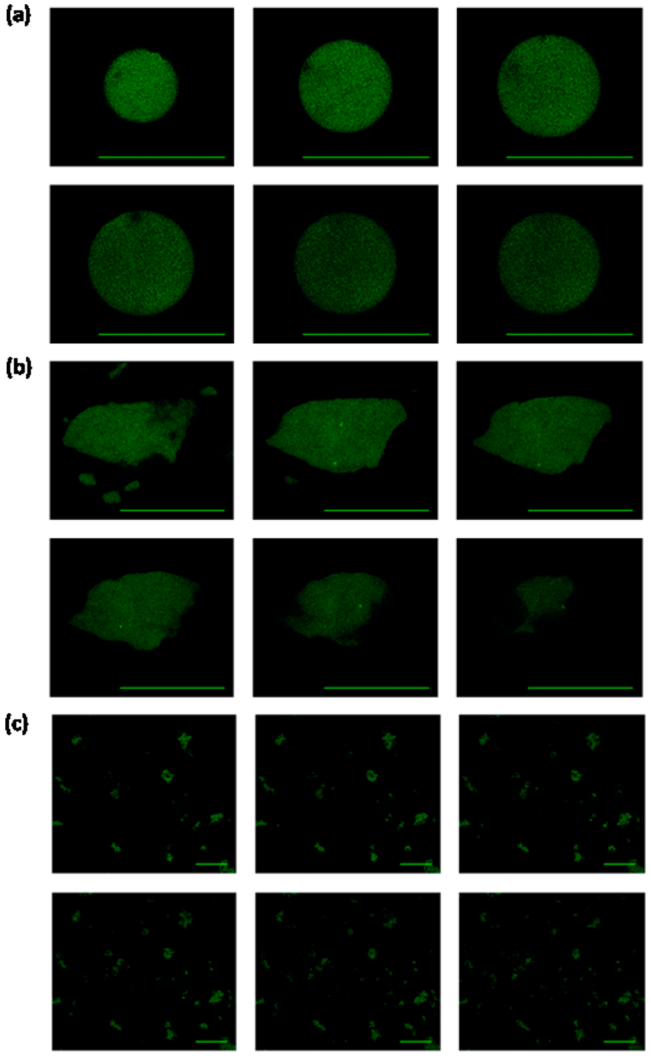

Figure 1. Confocal fluorescence images of Zbasic2_DAAO immobilized on silica supports: (a) CPG, (b) MSU-VLP, and (c) MSU-F. The scale bar indicates 100 μm in parts a and b and 20 μm in part c. Images were obtained by taking different z-section scans with 0.33 (c) and 4.99 μm (a, b) depth margins between images.

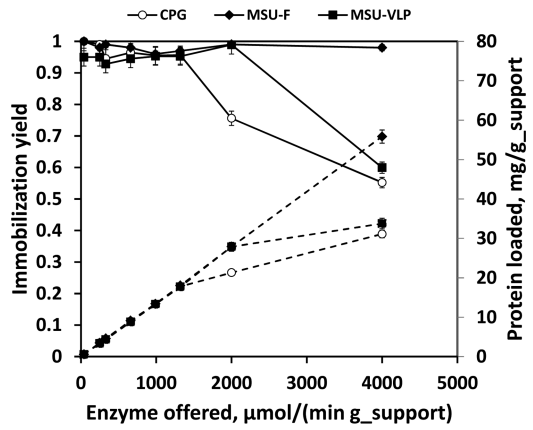

Figure 2. Immobilization of Zbasic2_DAAO on silica supports. Immobilization yield is the ratio of bound and initially offered enzyme activity. It is shown in solid lines. Dashed lines show the protein loaded on the support. The supports are indicated by symbols. For more detail, see the Experimental Section.

protein continued to be bound linearly proportionally to the amount offered. Note that because of the high selectivity of the immobilization, which is confirmed by analysis with SDS–PAGE of the protein detached from the supports under stringent elution conditions (data not shown), measurement of the bound protein actually represents the amount of Zbasic2_DAAO immobilized. When comparing the binding properties of three supports, it is worth noting that the amounts of activity and protein loadable were correlated with the declared specific surface areas of the support, which increases in the order CPG < MSU-VLP < MSU-F. However, there was no correlation between activity and protein loaded and the support's pore size. It is also interesting in view of the approximate molecular dimensions of the homodimeric DAAO (10 nm × 7 nm × 4.5 nm) that the average pore size of 17 nm in MSU-F was still sufficient to allow for enzyme immobilization in high yield (Figure 2).

To characterize the spatial distribution of Zbasic2_DAAO immobilized on the different supports, confocal laser scanning microscopy (CLSM) was used. The fluorescence of the protein-bound FAD cofactor can be detected conveniently without a requirement of additional labeling of the enzyme.[48,49] Figure 1 shows representative images collected from each support loaded at ∼1000 U/g_support. The microscopic evidence reveals that all parts of the solid supports were accessible to Zbasic2_DAAO. Remarkably, this is true even for MSU-F with its relatively narrow pores. Figure 1 and the accompanying Figure S2 in the Supporting Information also confirm a largely homogeneous distribution of the immobilized oxidase throughout the solid particle in each support.

In trying to establish performance-to-structure correlations for immobilized enzymes, it is crucial to detect heterogeneity or prove its absence in the internal enzyme distribution. Although often assumed to be homogeneous for the sake of simplicity, experimental evidence shows the opposite in various cases that, especially under conditions of fast adsorption the actual enzyme distribution on the solid surface, featured heterogeneity (e.g., preferred outer-sphere binding) to a large degree.[50] Figure S3 shows the immobilization time course of Zbasic2_DAAO on the different silica supports. On each support, binding of the enzyme required over 2 h to be complete. This relatively slow binding probably explains why immobilized enzyme was homogeneously distributed in the solid supports, even in the one having small pores (MSU-F). Moreover, MSU-F has the smallest particle size of the silica supports used. Therefore, this implies that diffusional distances during protein immobilization were the smallest for this material.

Characterization of Silica-Supported Immobilized Preparations of Zbasic2_DAAO. It is common for an immobilized enzyme that its actual activity is significantly lower than expected from the amount of activity bound to the insoluble support.[8,21,43] The ratio between the actual and bound activities is generally referred to as the effectiveness factor (η) of the immobilizate. Figure 3 shows results on analysis of the different Zbasic2_DAAO immobilizates in terms of η. In panel A is shown the dependence of the *actual* activity on the amount of activity offered. Contrary to the dependence of the *bound* activity on activity offered, which was linear for all supports up to a loading about 1300 U/g_support (Figure 2), dependence of the actual activity exhibited a pronounced curvature already at comparably low enzyme loadings. The effect of leveling out of the actual activity at high enzyme loadings was the strongest for CPG, but it was also clearly

DOI: 10.1021/acscatal.5b01601
ACS Catal. 2015, 5, 5984–5993

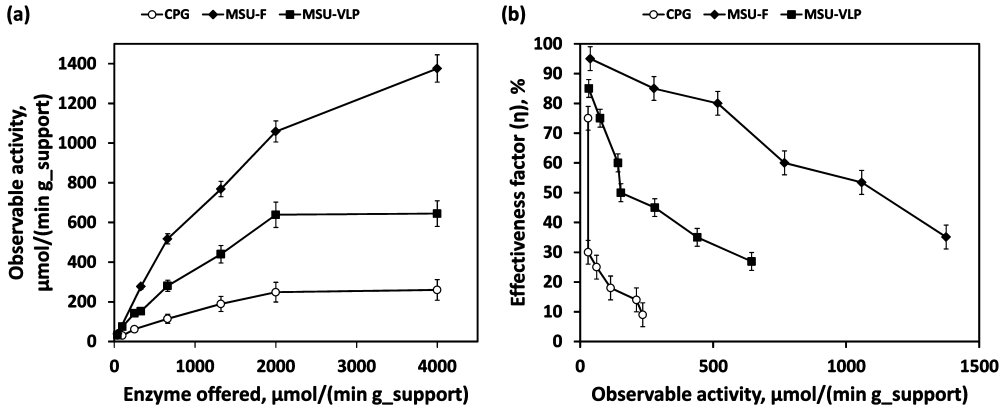

Figure 3. Observable activity (a) and catalytic effectiveness (b) of Zbasic2_DAAO immobilizates in the oxidation of D-Met. The observable activity represents the initial rate of O_2 consumption in bulk solution. The catalytic effectiveness is the ratio between the observable activity and the activity bound to the support. Bound activity is the product of immobilization yield and offered activity. Reactions were performed at 30 °C using air-saturated potassium phosphate buffer (50 mM; pH 8.0). For more detail, see the Experimental Section.

recognized for MSU-F. The maximum oxidase activity of CPG and MSU-VLP immobilizates was therefore ~200 U/g_support and 600 U/g_support, respectively. Using MSU-F, the maximum activity was not reached in the experiment, but a trend of approaching a "saturated" value was also noticeable for this support.

Panel B of Figure 3 compares the three silica supports according to the dependence of η on the immobilizate's actual activity. The overall trend of a decrease in η on an increase in activity was present in all supports, but there was a pronounced difference in the magnitude of the effect. For CPG, the drop in η was the most dramatic, resulting in <10% effectiveness ($\eta <$ 0.1) at a low actual activity of only ~250 U/g_support. The declining tendency of η was attenuated in the cellular foam silicas, more strongly so in MSU-F than in MSU-VLP. At a high level of activity, however, the η values of the two MSU supports appeared to gradually approach each other so that the two immobilizates became similarly effective. The immediate realization from these results was that MSU-L and, with certain qualifications, MSU-VLP are suitable choices for immobilization of Zbasic2_DAAO. CPG, by contrast, is completely unsuitable. However, why it was that enzyme immobilizates exhibited such distinctly different η–activity relationships was not clear from the structural characteristics of the silica supports used (Table S1). The effect therefore necessitated more detailed investigation. On the basis of evidence from CLSM analysis (Figure 1), varying degree of heterogeneity in enzyme distribution within the porous support was ruled out as an explanation of the differences between enzyme immobilizates. Moreover, judging from the value of η at very low actual activity, which was almost unity for the MSU-F immobilizate and still 0.75 for the CPG immobilizate (Figure 3, panel B), Zbasic2_DAAO had not lost a substantial amount of its intrinsic activity in immediate consequence of the attachment to either one of the three silica supports. Indirectly, as argued elsewhere in greater detail,[21,22] this result supported the suggestion that Zbasic2_DAAO binds to silica surfaces in a highly directed manner via its SBM. Also as proposed earlier,[21,22] this oriented binding mode manages to retain the intrinsic activity of the soluble enzyme in the solid immobilizate almost in full; hence, $\eta \approx 1$. An additional ramification is that differences in the η–activity relationship for the three immobilizates of Zbasic2_DAAO (Figure 3) do not originate from support-specific differences in the binding mode of the enzyme. A variable degree of diffusion limitation was therefore speculated to have caused the individual characteristics of the solid-supported enzyme preparations.

Luminophor Labeling of Silica Supports for Optical Sensing of O_2 in Heterogeneous Environment. To gain direct evidence on the actual availability of dissolved O_2 in the heterogeneous environment of the solid oxidase preparations, we considered an optical sensing approach previously used with enzymes immobilized on an organic polymer support. In this approach, tris(4,7-diphenyl-1,10-phenanthroline) ruthenium dichloride[42,43,51,52] ($Ru(dpp)_3$) was bound to the insoluble support, and quenching of the phosphorescence of the immobilized luminophor by O_2 constituted the principle of O_2 measurement.[41−43,52] Critical requirements for application of the method to silica supports were that labeling of the solid surface with $Ru(dpp)_3$ was homogeneous throughout the porous particle and that the luminophor was not leached in water. Optimization of the labeling conditions was necessary to avoid rapid aggregation of $Ru(dpp)_3$ in near-surface regions of the silica particles (Figure S4). Guided by evidence from CLSM analysis, as shown in Figure 4 and the accompanying Figure S5 in the Supporting Information, the ethanol cosolvent concentrations (10−50%, by volume) used during loading and washing of the support as well as the amount of luminophor loaded (1−5 mg/g_support) were adjusted such that a labeling with $Ru(dpp)_3$ on the internal surface of each of the three supports that was adequate both in *amount* and *uniformity of label distribution* for the intended sensing application was achieved.

When incubated under conditions of the enzymatic reaction (50 mM D-Met; pH 8.0; 30 °C; end-over-end mixing), release of luminophor from the silica supports was not detectable over 24 h. Using a high NaCl concentration (2 M) in the presence of Tween 80 (0.5%), however, immobilized $Ru(dpp)_3$ was washed off under regeneration of the free support, as shown by CLSM. We confirmed that labeling of the silica supports with $Ru(dpp)_3$ as optimized did not affect the subsequent immobilization of Zbasic2_DAAO regarding both the bound activity and the value of η. The alternative sequence of immobilization in which the enzyme is immobilized prior to labeling with $Ru(dpp)_3$ was not considered for reason because enzyme inactivation under the labeling conditions when both ethanol cosolvent and ruthenium luminophor were found was destabilizing for Zbasic2_DAAO.[43]

DOI: 10.1021/acscatal.5b01601
ACS Catal. 2015, 5, 5984−5993

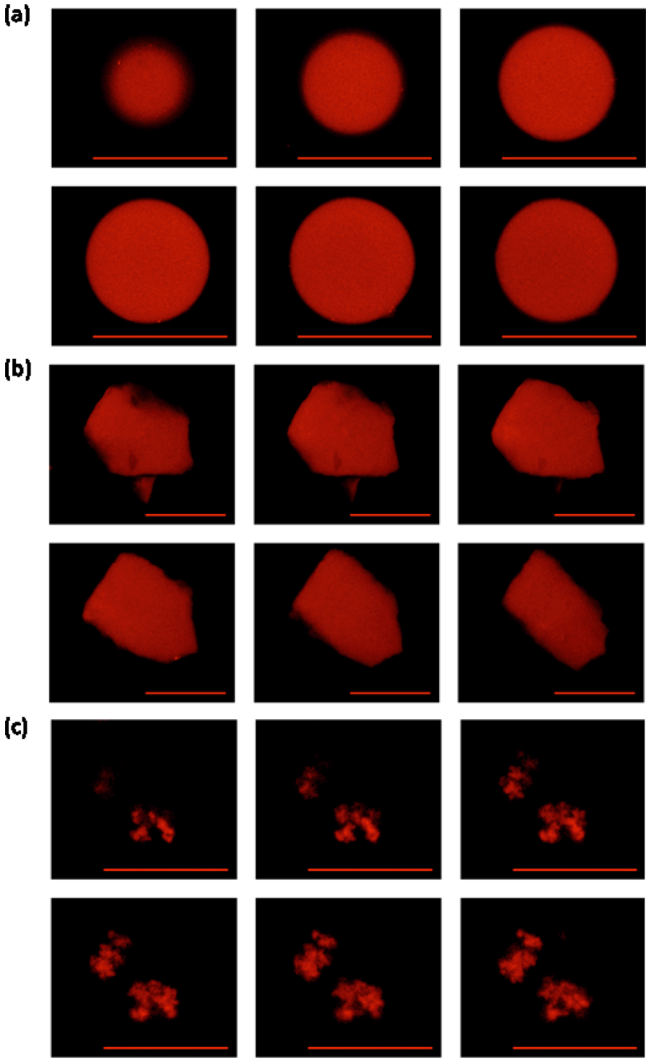

Figure 4. Confocal fluorescence images of silica supports labeled with $Ru(dpp)_3$. (a) CPG; (b) MSU-VLP; (c) MSU-F. The scale bar indicates 100 μm in (a) and (b), and 20 μm in (c). Images were obtained by taking different z-section scans with a 0.33 μm (c) and a 4.99 μm (a, b) depth margin between each image.

To evaluate the labeled supports for O_2 sensing, luminescence lifetime measurements according to the phase modulation technique[41−43,52] were performed from stirred suspensions of silica particles containing immobilized Zbasic2_DAAO. Figure S6 provides calibration of the analytical signal from each of the three silica supports, showing good correlation between the measured lifetime and the steady-state O_2 concentration. A dynamic range between the approximate limit of quantification of 5 μM and the air-saturated concentration of 250 μM, which was the maximum O_2 concentration used in further experiments, was established for the analytical method. Figure S4 also shows that the labeled silica supports differed in sensitivity in the order MSU-F > MSU-VLP > CPG. Differences in the mass-related surface area of the silica supports (Tables S1, S2) probably accounted for the effect. The response time of the solid sensor particles was evaluated in assays in which consumption of O_2 due to oxidation of L-lactate by soluble L-lactate oxidase was measured. The $[O_2]$ time course recorded from solid particles was compared to a reference time course measured directly from the liquid phase using a fiber-optic sensor. The loading of L-lactate oxidase in solution was varied to change the enzymatic reaction rate. Figure S7 shows that the two corresponding $[O_2]$ time courses were superimposable for each silica support under all conditions used. Therefore, the response time of the solid sensor particles was fast enough to avoid a time delay in collecting data from the heterogeneous environment relative to the homogeneous liquid phase.

The signal-to-noise ratio constitutes a technical detail of the measurement, which we refer to here only briefly. Using particles loaded with $Ru(dpp)_3$ in a mass ratio of 2.5 mg/g_support and applying these particles in a suspended concentration of 2.5 mg_support/mL, luminescence lifetime measurements were of high quality. Lowering the amount of luminophor loaded or working at a decreased particle concentration generally resulted in a decrease in the signal-to-noise ratio. In summary, these results demonstrate how the methodological principle of internal sensing of molecular oxygen in porous materials can be extended from organic polymeric supports, to which it was originally restricted, to the highly important class of silica supports. The scope of the application of the analytical method in heterogeneous biocatalysis but also heterogeneous chemical catalysis of O_2-dependent transformations is therefore broadened significantly.[27,34] With mesoporous silica materials, an emerging type of catalytic support is included.

Measurement of the Internal Availability of O_2 during the Heterogeneous Enzymatic Reaction Reveals Effects of Diffusional Limitation. Whenever substrate diffusion is rate-limiting in heterogeneously catalyzed reactions, the steady-state substrate concentration in the liquid bulk phase will be higher than the corresponding substrate concentration at a given spatial point in the solid support. The kinetic consequences of substrate depletion from the heterogeneous environment therefore need to be considered for optimization of an immobilized enzyme. In the case of Zbasic2_DAAO, the enzymatic reaction is kinetically first-order with respect to the O_2 concentration, implying that any change in the internal $[O_2]$ will proportionally affect the enzymatic rate ("activity"). Experiments were therefore performed to evaluate the $[O_2]$ gradients between the bulk phase and the *space-averaged* solid phase during reactions catalyzed by different Zbasic2_DAAO immobilizates on the $Ru(dpp)_3$-labeled silica support. The reader is advised to note the space-averaged nature of luminescence lifetime determinations from the solid particles. The measured $[O_2]$ constitutes an averaged concentration over the characteristic particle dimension (e.g., radius of the spheric CPG). Importantly, therefore, the used silica supports were all highly transparent throughout.

Figure 5 shows comparison of time-resolved $[O_2]$ profiles in the external and internal environment of different immobilized oxidase preparations. Major differences between the three silica supports are revealed as a result. Using CPG (panel A), a large $[O_2]$ gradient ($\Delta[O_2]$) was formed between liquid bulk and solid support in dependence of reaction time. Note that the decrease in the bulk O_2 concentration occurred because gas−liquid O_2 transfer by surface aeration was not significant under these conditions. The enzymatic reaction rate (r_{obs}) was therefore obtained from the data collected from the bulk phase. The $\Delta[O_2]$ increased in clear dependence on the bound oxidase activity (Figure S8), and it was a maximum shortly after the substrate addition. The course of $[O_2]$ in the solid support involved a fast initial decrease of the O_2 level that was followed

DOI: 10.1021/acscatal.5b01601
ACS Catal. 2015, 5, 5984−5993

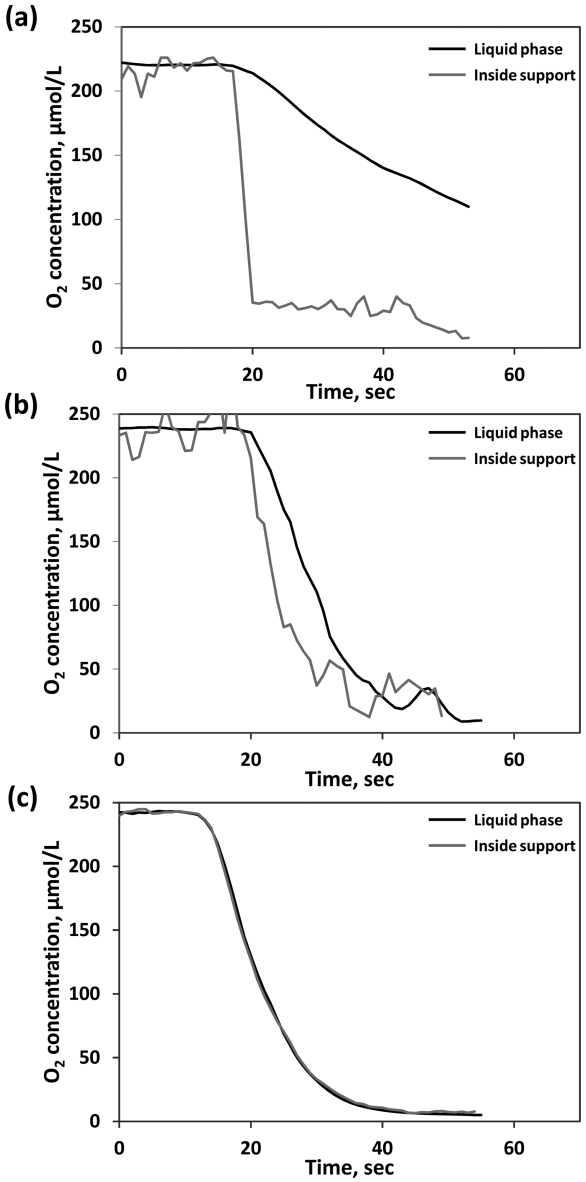

Figure 5. Time courses of the O_2 concentration in liquid phase and inside porous support during oxidation of D-Met by different Zbasic2_DAAO immobilizates. Each support was loaded with 600 μmol/(min g_carrier), and 5 mg_carrier/mL was used in the reaction. (a) CPG; (b) MSU-VLP; (c) MSU-F. Reactions were performed at 30 °C using air-saturated potassium phosphate buffer (50 mM; pH 8.0). For more detail, see the Experimental Section.

by a comparably slower O_2 consumption. The second kinetic phase probably reflected the steady state where the rates of O_2 transport into the support and heterogeneous enzymatic reaction had become equal. The maximum value of $\Delta[O_2]$ was determined from the time-resolved $[O_2]$ profiles of different CPG immobilizates, which as a result of the variation in the amount of enzyme loaded gave r_{obs} values in the range 5−250 μmol/(min g_support). Figure 6 shows that $\Delta[O_2]$ increased dramatically as a consequence of the increase in r_{obs} (panel A) and that η increased as $\Delta[O_2]$ was lowered (panel B).

Used as immobilization supports, the two cellular foam silicas exhibited a behavior pronouncedly different from that of CPG, as shown in Figure 5. Compared at equivalent loadings of enzyme activity, the development of $\Delta[O_2]$ relative to CPG was strongly attenuated in MSU-VLP, and it was almost completely absent in MSU-F ($\Delta[O_2] \leq 10\%$ air saturation). In other words, Zbasic2_DAAO immobilized on MSU-F, and with some qualifications on MSU-VLP, operated in a nearly "pseudohomogeneous" environment regarding the availability of molecular oxygen for the enzymatic reaction under the conditions used. Employing MSU-VLP as demonstrated in Figure 6 and the accompanying Figure S9 in the Supporting Information, an increase in the enzyme loading resulted in a gradual increase in the magnitude of the O_2 gradient formed in the enzymatic reaction. The maximum value of $\Delta[O_2]$ increased in response to an increase in r_{obs}. As seen with CPG, the value of η of the enzyme immobilizate of MSU-VLP increased strongly as a consequence of a progressing avoidance of a drop in the internal O_2 concentration at low r_{obs} (Figure 6, panel B). Diffusional limitations are therefore revealed clearly for the MSU-VLP immobilizates, but they are by far less severe than they are in CPG immobilizates. However, in both MSU-VLP and CPG, the observed $\Delta[O_2]$ explained quantitatively the declining tendency of η in response to an increased loading of enzyme (Figure 3).

The MSU-F immobilizates presented a special case in which, as shown in Figure 6 (panel A) and the accompanying Figure S10 in the Supporting Information, the $\Delta[O_2]$ never reached a significant value, irrespective of the change in r_{obs} between 5−800 μmol/(min g_support). A tiny drop of the O_2 concentration in the solid support appeared to have occurred (≤10% of the value at air saturation; Figure 6A), but it was always at the very limit of resolution of the analytical method (Figure S8). Therefore, this result implies that the MSU immobilizate was not affected by the O_2 diffusion limitation in the range of enzyme loadings examined. That η still decreased at enzyme loadings of 600 μmol/(min g_support) or higher (Figure 3) clearly indicates that the intrinsic activity of Zbasic2_DAAO was affected by the immobilization under these conditions. Investigation of the cause of the effect was beyond the scope of this study, but we note that it may equally involve protein concentration-dependent processes on the solid surface and in solution.[53] One possibility is that the surface properties (e.g., hydrophobicity) change in response to an increasing enzyme loading and that such change impacts the enzyme activity. The effects of surface crowding could also be involved.

Heterogeneously Catalyzed Oxidative Deamination of D-Met by Zbasic2_DAAO on Different Silica Supports. We finally examined the three Zbasic2_DAAO immobilizates, each loaded to an activity of 600 μmol/(min g_support), in repeated batchwise conversions of D-Met that involved complete recycling of the solid catalyst after each round of reaction. Surface aeration in combination with suitable catalyst loading was used to ensure that O_2 saturation in the bulk was near saturation throughout. Figure 7 shows time courses of the heterogeneously catalyzed reactions and compares them with the reaction catalyzed by a soluble enzyme. In each reaction, production of α-keto acid product was approximately linear with time. The productivity increased in the order CPG < MSU-VLP (2-fold) < MSU-F (1.3-fold), as expected from the immobilizates' effectiveness factors (Figure 3 and 6). The productivity of the MSU-F immobilizate was just around 10% less than that of the soluble enzyme, indicating an almost perfectly effective immobilized biocatalyst. All solid catalysts were easily separated from the liquid phase by gravity

DOI: 10.1021/acscatal.5b01601
ACS Catal. 2015, 5, 5984−5993

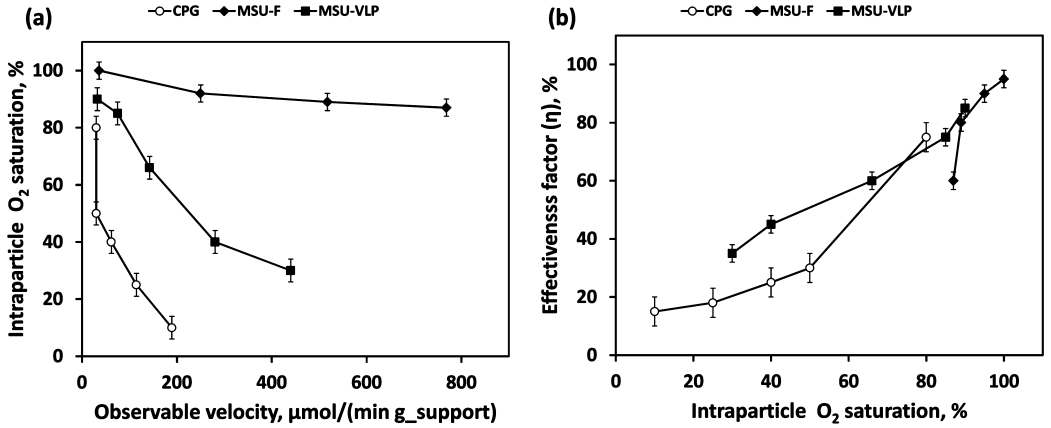

Figure 6. (a) Dependence of the O_2 concentration inside the porous support (at apparent steady state) on the observable velocity of D-Met oxidation by the Zbasic2_DAAO immobilizate, and (b) dependence of the effectiveness factor of the immobilizate on the O_2 concentration inside the porous support. Reactions were performed at 30 °C using air-saturated potassium phosphate buffer (50 mM; pH 8.0). For more detail, see the Experimental Section.

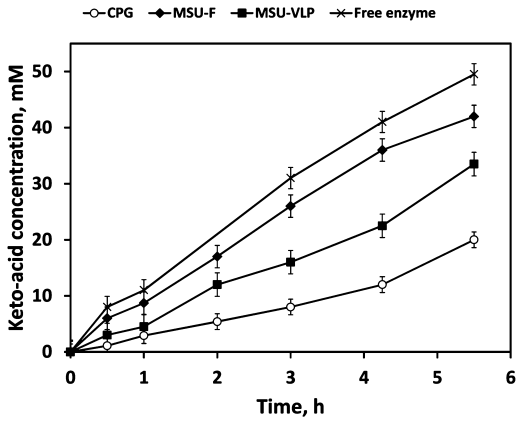

Figure 7. Batchwise oxidation of D-Met (50 mM) into 2-keto-4-(methylthio)butyric acid using soluble or silica-supported preparations of Zbasic2_DAAO at equivalent volumetric enzyme loadings of 0.2 μmol/(min mL). Catalase (400 U/mL) was added to destroy H_2O_2, to partly regenerate O_2, and to prevent α-keto acid decarboxylation. The symbols indicate soluble enzyme (asterisk) and immobilizates on CPG (open circles), MSU-VLP (squares), and MSU-F (diamonds). Note that immobilizates were recycled for two new rounds of reaction, giving the same performance each time. For more detail, see the Experimental Section.

sedimentation, and they could be recycled at least three times without an appreciable loss in enzyme activity.

CONCLUSIONS

A method of optical sensing of O_2 in the liquid phase within porous silica materials was developed. The effect of diffusion limitation in silica-supported immobilizates of Zbasic2_DAAO was thus made evident directly from experiment. The consequent ability to dissect the main observable of the immobilization (η) into its principal factors, that is, the biocatalytic reaction and the physical transport of O_2, provides a fundamentally advanced approach to the rational development of silica-supported, immobilized, O_2-dependent biocatalyst. In particular, the selection among different candidate solid supports was made possible specifically targeted to the intensification of O_2 mass transport. Direct evidence on the internal (heterogeneous) environment of the immobilized Zbasic2_DAAO was absolutely essential in the process, for simple particle parameters such as average pore size and particle diameter exhibited a complex correlation with the behavior of the enzyme immobilizates. Huge differences in the silica supports examined herein emphasized the high importance of evidence-based selection of the support material. Compared with standard CPG, enhanced mass transfer in MSU-F resulted in enlargement of the available process window for immobilized Zbasic2_DAAO minimally by ~1 order of magnitude. The MSU-F immobilizate approached perfection of a heterogeneous biocatalyst in being almost as effective as a free enzyme. Overall, the study uses the example of Zbasic2_DAAO to develop a generally applicable design of an O_2-dependent biocatalyst on underivatized porous silica support. Oriented immobilization via the Zbasic2 silica-binding module is employed to create a solid enzyme preparation that offers high intrinsic activity and can be recycled easily. Internal O_2 sensing enables targeted optimization of the immobilizate, particularly regarding the degree of diffusional limitation.

EXPERIMENTAL SECTION

Materials. Chimera of D-amino acid oxidase (from *Trigonopsis variabilis*) containing Zbasic2 fused to the enzyme's N-terminus was used. Construction, isolation, and characterization of Zbasic2_DAAO were reported recently.[23] *Aerococcus viridans* L-lactate oxidase was a kind gift from Roche Diagnostics (Penzberg, Germany). D-Met, 4-aminoantipyrine, *N*,*N*-dimethylaniline, 2,4-dinitrophenylhydrazine, peroxidase from horseradish, and glucose oxidase (type II-S, 15000–50000 units/g_solid) from *Aspergillus niger* were from Sigma-Aldrich GmbH (Vienna, Austria). Dichloride (4,7-diphenyl-1,10-phenantroline)ruthenium(II) ($Ru(dpp)_3$) was from ABCR GmbH (Karlsruhe, Germany). Glucose was from Roth (Karlsruhe, Germany). Controlled pore glass (Trisoperl; CPG) was from Vitra Bio GmbH (Steinach, Germany). Mesostructured (cellular foam) silicas MSU-VLP and MSU-F were from InPore Technologies/DBA Claytec, Inc. (East Lansing, MI, USA). Unless otherwise mentioned, all chemicals were from Sigma (Vienna, Austria) and of analytical grade.

Enzyme Assays. The activity of soluble or immobilized DAAO was determined using a peroxidase-coupled assay.[21,23] Direct measurement of the O_2 consumption rate (r_{O_2}) was alternatively used for activity determination.[43] Assays were performed at 30 °C in 50 mM air-saturated potassium

DOI: 10.1021/acscatal.5b01601
ACS Catal. 2015, 5, 5984–5993

phosphate buffer, pH 8.0, using 10 mM D-Met as the substrate. The r_{O_2} was measured with a fiber-optic microoptode (Pyroscience GmbH, Aachen, Germany) connected to a fiber-optic oxygen meter (model Firesting, Pyroscience). One unit of enzyme activity is the amount of DAAO that produces 1 μmol of H_2O_2/min or consumes 1 μmol of O_2/min at the conditions used. The enzyme preparations used had specific activities between 3 μmol/(min mg_protein) for crude cell extract and 70 μmol/(min mg_protein) for purified enzyme.

Luminophor Labeling of Silica Supports. Silica particles were washed with 50 mM potassium phosphate buffer, pH 7.0. The $Ru(dpp)_3$ stock solution in ethanol (2.5 mg/mL) was diluted 2-fold with buffer and incubated with silica at the concentrations indicated using an end-over-end rotator (20 rpm) for mixing at room temperature (~25 °C). The particle suspension was diluted stepwise with buffer to 10% ethanol and then incubated for 1.5 h under magnetic stirring just strong enough to keep the particles stirred up. Finally, the supports were thoroughly washed with buffer and stored at 4 °C until further use.

Immobilization of Zbasic2_DAAO. Potassium phosphate buffer, pH 8.0, containing 1.0 M NaCl and 0.5% (by volume) Tween 20 was used.[22] The immobilization mix contained 50 mg of well-washed silica support in a total liquid volume of 1 mL. In addition to buffer, the supernatant contained a varied amount of *Escherichia coli* cell extract containing Zbasic2_-DAAO. The used enzyme activity varied between 0.05 and 200 U. The protein concentration was between 0.02 and 60 mg/mL. The pH of 8.0 was controlled after addition of enzyme and was set when necessary. Binding to the silica support was determined from a decrease in activity and protein in solution (supernatant, wash solutions). Immobilization yield is the ratio of activity or protein bound and initially offered. Immobilization to silica proceeded until no further decrease in the supernatant occurred. The solid material was then washed with buffer (0.5 M NaCl but no Tween 80; pH 8.0) for 1 h using gentle mixing in the rotator. A second washing was identically performed using buffer containing Tween 80 (0.5%, by volume) but no NaCl. Immobilizates were stored in 50 mM potassium phosphate buffer, pH 7.0, at 4 °C. Note that enzyme immobilization on $Ru(dpp)_3$-labeled silica involved buffer containing reduced amounts of NaCl (0.25 M) and Tween 20 (0.01%). The reason was to avoid leaching of the luminophor.

Determination of Catalytic Effectiveness of Immobilized Preparations of Zbasic2_DAAO. The parameter η describes the ratio between the observable activity of the immobilizate and the activity the immobilizate is expected to have from the amount of activity bound to the support. Both activities are expressed in micromoles/(minute grams_support). The observable activity was determined as the O_2 consumption rate during conversion of D-Met, measured with a fiber-optic oxygen microoptode (Pyroscience GmbH, Aachen, Germany). Between 0.5 and 25 mg of enzyme immobilizate were resuspended in 4 mL of air-saturated potassium phosphate buffer (50 mM; pH 8.0). An open glass vial (1.2 cm diameter) was placed in a water bath (30 °C), and magnetic stirring (6 × 3 mm; 300 rpm) was used. The reaction was started by adding 200 μL of substrate solution (200 mM D-Met) once the O_2 measurement gave a stable signal. A decrease in the O_2 was typically followed for about 5 min. It was confirmed by visual inspection that under the stirring conditions used, the silica particles were kept completely in suspension and were not mechanically destroyed during the course of the experiment. In addition, the enzyme immobilizate was retained and could be reused for another round of activity measurement. Successive activity measurements gave fully consistent results. Figure S12 in the Supporting Information shows the results of an analysis by CLSM in which particles before and after performing a stirring experiment were analyzed.

Determination of Internal O_2 Concentration in Labeled Silica Supports. A phosphorescent signal of labeled silica particles containing or lacking immobilized Zbasic2_-DAAO was detected by phase-shift measurements using a miniaturized lock-in amplifier (pH-Mini, Presens GmbH, Regensburg, Germany) equipped with a 2 mm optical fiber interfaced with the reactor.[42,43] Measurements consisted of the determination of the phase shift of the emitted light signal after excitation of the O_2-sensitive $Ru(dpp)_3$ indicator by a sinusoidally intensity-modulated light. The phase shift was caused by dynamic luminescence quenching of the indicator, depending on the O_2 concentration. Measurements were carried out at a modulation frequency of 45 kHz. The stirred reactor setup and the conditions were the same as above, except that particle loading was typically between 0.5 and 5.0 mg/mL. Useful signal-to-noise ratios were thus obtained. It was verified through visual inspection that particles were not mechanically destroyed in the time span of the experiment. The reaction was started through substrate addition once the system gave a stable phase shift signal, and the change of phase shift was monitored over time. The Stern−Volmer model was applied to relate experimental phase shifts (and the corresponding phosphorescence lifetimes) on the O_2 concentration. Calibration of the phase shift response was done for each immobilizate separately, as shown in the Supporting Information. Phase shift measurements at various defined O_2 concentrations (adjusted by bubbling with N_2) were performed. The response time of the labeled silica particles was evaluated in experiments in which soluble L-lactate oxidase (0.25−25 ng/mL) consumed O_2 in bulk as a result of L-lactate (50 mM), and the resulting decrease in O_2 was monitored through the particle-based phase shift measurement as well as directly in the bulk using the oxygen microsensor described above.

Confocal Laser Scanning Microscopy of Immobilized Zbasic2_DAAO and Labeled Silica Supports. About 30 μL of luminophor-labeled and enzyme-immobilized silica support (10 mg/mL) suspended in 50 mM potassium phosphate buffer, pH 7.0, was placed on a microscope slide mounted with a coverslip. Confocal images were acquired using a Leica DM5500Q microscope system (Mannheim, Germany) equipped with an objective for 63-fold magnification (ACS APO 63×/1.30 OIL). For imaging of the flavin cofactor of Zbasic2_DAAO, excitation was at 405 nm, and emitted light was collected in the range 480−650 nm. The imaging analysis cannot distinguish between protein-bound and free FAD attached to the solid surface. It is important to note, therefore, that imaging was always performed immediately after the immobilization, thus eliminating the possibility that substantial amounts of FAD could have been released from the protein onto the solid surface as a result of progressing protein denaturation during immobilization and storage. Both the free and the immobilized enzyme were fully stable during the timespan of the experiment. In addition, immobilized Zbasic2_DAAO was shown to have a high intrinsic activity approaching that of the free enzyme. Because dissociation of

DOI: 10.1021/acscatal.5b01601
ACS Catal. 2015, 5, 5984−5993

FAD results in enzyme inactivation, evidence of high intrinsic activity refutes release of cofactor in substantial amounts. $Ru(dpp)_3$ imaging and excitation were at 488 nm, and the emitted light was collected in the range 500−694 nm. Images were processed using Fiji imageJ processing package software. Bright field pictures were acquired using a Leica DFC360FX CCD camera connected to the microscope.

Repeated Batchwise Oxidation of D-Met by Immobilizates of Zbasic2_DAAO Using Recycling of Solid Catalyst. Reactions consisted of 1 mL of solution (50 mM D-Met; 50 mM potassium phosphate, pH 8.0) containing 0.33 mg of immobilizate/mL (bound activity: 600 U/g_support) or 0.2 U/mL of free enzyme. Catalase from bovine liver (4000 U/mg) was added at 0.1 mg of protein/mL to ensure the decomposition of hydrogen peroxide formed.[54] Incubation was performed in Eppendorf tubes at room temperature (~25 °C), and an end-over-end-rotator (20 rpm) was used for mixing. O_2 availability in supernatant (~90% air saturation at atmospheric pressure) was regularly checked using measurement with the oxygen microoptode. At indicated times, a homogeneous sample was withdrawn, and the concentration of 2-keto-4-(methylthio)butyric was determined. Reaction progress was followed for 6 h. At the end, the enzyme immobilizate was recovered by sedimentation, and it was used again for two new rounds of conversion. Quantification of 2-keto-4-(methylthio)-butyric was performed as described elsewhere[55,56] with some modifications. Briefly, 50 μL of sample and the same volume of 2,4-dinitrophenylhydrazine (DNP) solution (1.0 mM of DNP in 2 M HCl) were mixed and incubated at room temperature for 10 min. Subsequently, 200 μL of 1.5 M NaOH was added, and the mixture was mixed and incubated for an additional 10 min. Finally, 200 μL of the mixture was diluted in the same volume of 50 mM potassium phosphate, pH 7.0, and the absorbance was read at 440 nm. A blank was also measured under the same conditions but using 50 mM D-Met in 50 mM potassium phosphate, pH 8.0, instead of the sample solution.

Data Analysis and Presentation. The data shown are averages of three or more independent experiments. Mean values and their standard deviations are given in the text and figures.

■ ASSOCIATED CONTENT

Supporting Information

The Supporting Information is available free of charge on the ACS Publications website at DOI: 10.1021/acscatal.5b01601.

A summary of properties of the silica supports used (Table S1 and S2); supporting scanning electron microscope images of the supporting mesocellular foams supports used (Figure S1); supporting CLSM images of Zbasic2_DAAO immobilized on the different silica supports (Figure S2); time courses of immobilization of Zbasic2_DAAO on the different silica supports (Figure S3); supporting CLSM images showing aggregation of ruthenium luminophor in the CPG support (Figure S4); supporting CLSM images showing immobilization of ruthenium luminophor on the different silica supports (Figure S5); Stern−Volmer plot correlating luminescence lifetime recorded from labeled silica supports and the O_2 concentration in bulk liquid (Figure S6); response time analysis of labeled silica supports under conditions of O_2-dependent enzymatic reaction in solution (Figure S7); time-resolved profiles of O_2 concentration in the bulk liquid phase and in solid particle for reactions by Zbasic2_DAAO immobilized on CPG (Figure S8), MSU-VLP (Figure S9) and MSU-F (Figure S10); determination of the maximum value of ΔO_2 in reactions catalyzed by different DAAO immobilizates (Figure S11); supporting CLSM images comparing silica supports before and after use in stirring experiments (Figure S12) (PDF)

■ AUTHOR INFORMATION

Corresponding Author

*Phone: +43 316 873 8400. Fax: +43 316 873 8434. E-mail: bernd.nidetzky@tugraz.at.

Notes

The authors declare no competing financial interest.

■ ACKNOWLEDGMENTS

Dr. Zdenek Petrasek (Institute of Biotechnology and Biochemical Engineering) assisted the CLSM experiments, and Prof. Thomas J. Pinnavaia (InPore Technologies/DBA Claytec, Inc) provided technical data about the silica supports used. Dr. Victoria Gascon (Molecular Sieves group, Institute of Catalysis and Petrochemistry, CSIC, Madrid, Spain) is thanked for structural characterization of the mesocellular foam supports used.

■ REFERENCES

(1) Torrelo, G.; Hanefeld, U.; Hollmann, F. *Catal. Lett.* **2015**, *145*, 309−345.
(2) Clouthier, C. M.; Pelletier, J. N. *Chem. Soc. Rev.* **2012**, *41*, 1585−1605.
(3) Guisán, J. M. *Immobilization of Enzymes and cells*; Humana Press: Totowa, NJ, 2010; pp 1−13.
(4) Buchholz, K.; Kasche, V.; Bornscheuer, U. T. *Biocatalysts and Enzyme Technology*; Wiley-VCH: Weinheim, 2005; pp 243−282.
(5) Hanefeld, U.; Cao, L.; Magner, E. *Chem. Soc. Rev.* **2013**, *42*, 6211−6212.
(6) Tran, D. N.; Balkus, K. J. *ACS Catal.* **2011**, *1*, 956−968.
(7) Liese, A.; Hilterhaus, L. *Chem. Soc. Rev.* **2013**, *42*, 6236.
(8) Garcia-Galan, C.; Berenguer-Murcia, Á.; Fernandez-Lafuente, R.; Rodrigues, R. C. *Adv. Synth. Catal.* **2011**, *353*, 2885−2904.
(9) Cantone, S.; Ferrario, V.; Corici, L.; Ebert, C.; Fattor, D.; Spizzo, P.; Gardossi, L. *Chem. Soc. Rev.* **2013**, *42*, 6262−6276.
(10) Sheldon, R. A.; van Pelt, S. *Chem. Soc. Rev.* **2013**, *42* (15), 6223−6235.
(11) Rodrigues, R. C.; Ortiz, C.; Berenguer-Murcia, Á.; Torres, R.; Fernández-Lafuente, R. *Chem. Soc. Rev.* **2013**, *42* (15), 6290−6307.
(12) Magner, E. *Chem. Soc. Rev.* **2013**, *42*, 6213−6222.
(13) Carlsson, N.; Gustafsson, H.; Thörn, C.; Olsson, L.; Holmberg, K.; Åkerman, B. *Adv. Colloid Interface Sci.* **2014**, *205*, 339−360.
(14) Hartmann, M.; Kostrov, X. *Chem. Soc. Rev.* **2013**, *42*, 6277−6289.
(15) Hartmann, M. *Chem. Mater.* **2005**, *17*, 4577−4593.
(16) Gaffney, D.; Cooney, J.; Magner, E. *Top. Catal.* **2012**, *55*, 1101−1106.
(17) Zhou, Z.; Hartmann, M. *Chem. Soc. Rev.* **2013**, *42*, 3894−3912.
(18) Gascón, V.; Díaz, I.; Márquez-Álvarez, C.; Blanco, R. M. *Molecules* **2014**, *19*, 7057−7071.
(19) Bernal, C.; Sierra, L.; Mesa, M. *ChemCatChem* **2011**, *3*, 1948−1954.
(20) Bernal, C.; Illanes, A.; Wilson, L. *Langmuir* **2014**, *30*, 3557−3566.
(21) Bolivar, J. M.; Nidetzky, B. *Biotechnol. Bioeng.* **2012**, *109*, 1490−1498.
(22) Bolivar, J. M.; Nidetzky, B. *Langmuir* **2012**, *28*, 10040−10049.

DOI: 10.1021/acscatal.5b01601
ACS Catal. 2015, 5, 5984−5993

(23) Wiesbauer, J.; Bolivar, J. M.; Mueller, M.; Schiller, M.; Nidetzky, B. *ChemCatChem* **2011**, *3*, 1299−1303.
(24) Ikeda, T.; Kuroda, A. *Colloids Surf., B* **2011**, *86*, 359−363.
(25) Ikeda, T.; Motomura, K.; Agou, Y.; Ishida, T.; Hirota, R.; Kuroda, A. *Protein Expression Purif.* **2011**, *77*, 173−177.
(26) Sheldon, R. A.; Arends, I. W. C. E.; Ten Brink, G.-J.; Dijksman, A. *Acc. Chem. Res.* **2002**, *35*, 774−781.
(27) Sheldon, R. A. *Catal. Today* **2015**, *247*, 4−13.
(28) Shi, Z.; Zhang, C.; Tang, C.; Jiao, N. *Chem. Soc. Rev.* **2012**, *41*, 3381−3430.
(29) Podgoršek, A.; Zupan, M.; Iskra, J. *Angew. Chem., Int. Ed.* **2009**, *48*, 8424−8450.
(30) Chen, B.-T.; Bukhryakov, K. V.; Sougrat, R.; Rodionov, V. O. *ACS Catal.* **2015**, *5*, 1313−1317.
(31) Schümperli, M. T.; Hammond, C.; Hermans, I. *ACS Catal.* **2012**, *2*, 1108−1117.
(32) Que, L.; Tolman, W. B. *Nature* **2008**, *455*, 333−340.
(33) Punniyamurthy, T.; Velusamy, S.; Iqbal, J. *Chem. Rev.* **2005**, *105*, 2329−2363.
(34) Mallat, T.; Baiker, A. *Chem. Rev.* **2004**, *104*, 3037−3058.
(35) Davis, S. E.; Ide, M. S.; Davis, R. J. *Green Chem.* **2013**, *15*, 17−45.
(36) Hollmann, F.; Arends, I. W. C. E.; Buehler, K.; Schallmey, A.; Bühler, B. *Green Chem.* **2011**, *13*, 226−265.
(37) Turner, N. J. *Chem. Rev.* **2011**, *111*, 4073−4087.
(38) Monti, D.; Ottolina, G.; Carrea, G.; Riva, S. *Chem. Rev.* **2011**, *111*, 4111−4140.
(39) Hall, M.; Bommarius, A. S. *Chem. Rev.* **2011**, *111*, 4088−4110.
(40) Bolivar, J. M.; Eisl, I.; Nidetzky, B. *Catal. Today*; in press, 10.1016/j.cattod.2015.05.004.
(41) Bolivar, J. M.; Consolati, T.; Mayr, T.; Nidetzky, B. *Trends Biotechnol.* **2013**, *31*, 194−203.
(42) Bolivar, J. M.; Consolati, T.; Mayr, T.; Nidetzky, B. *Biotechnol. Bioeng.* **2013**, *110*, 2086−2095.
(43) Bolivar, J. M.; Schelch, S.; Mayr, T.; Nidetzky, B. *ChemCatChem* **2014**, *6*, 981−986.
(44) Pollegioni, L.; Molla, G.; Sacchi, S.; Rosini, E.; Verga, R.; Pilone, M. S. *Appl. Microbiol. Biotechnol.* **2008**, *78*, 1−16.
(45) Linssen, T.; Cassiers, K.; Cool, P.; Vansant, E. F. *Adv. Colloid Interface Sci.* **2003**, *103* (2), 121−147.
(46) Pilone, M. S.; Pollegioni, L. *Biocatal. Biotransform.* **2002**, *20* (3), 145−15 (42) (46).
(47) Turner, N. J. *Chem. Rev.* **2011**, *111* (7), 4073−4087.
(48) Tanaka, F.; Tamai, N.; Yamazaki, I.; Nakashima, N.; Yoshihara, K. *Biophys. J.* **1989**, *56*, 901−909.
(49) van den Berg, P. A. W.; Visser, A. J. W. G. In *New Trends in Fluorescence Spectroscopy Applications to Chemical and Life Sciences*; Valeur, B., Brochon, J.-C., Eds; Springer Berlin Heidelberg: Berlin, Heidelberg, 2001; pp 457−459.
(50) Bolivar, J. M.; Hidalgo, A.; Sánchez-Ruiloba, L.; Berenguer, J.; Guisán, J. M.; López-Gallego, F. *J. Biotechnol.* **2011**, *155*, 412−420.
(51) Quaranta, M.; Borisov, S. M.; Klimant, I. *Bioanal. Rev.* **2012**, *4*, 115−157.
(52) Papkovsky, D. B.; Dmitriev, R. I. *Chem. Soc. Rev.* **2013**, *42*, 8700−8732.
(53) Secundo, F. *Chem. Soc. Rev.* **2013**, *42*, 6250−6261.
(54) Hernandez, K.; Berenguer-Murcia, A.; Rodrigues, R. C.; Fernandez-Lafuente, R. *Curr. Org. Chem.* **2012**, *16* (22), 2652−2672.
(55) Oguri, S.; Watanabe, K.; Nozu, A.; Kamiya, A. *Food Chem.* **2007**, *100*, 616−622.
(56) Nuutinen, J. T.; Timonen, S. *Mycol. Res.* **2008**, *112*, 1453−1464.

DOI: 10.1021/acscatal.5b01601
ACS Catal. 2015, 5, 5984−5993